Applied Physics Letters

# Thermo-mechanical aspects of gamma irradiation effects on GaN HEMTs

Cite as: Appl. Phys. Lett. **120**, 124101 (2022); https://doi.org/10.1063/5.0087209
Submitted: 02 February 2022 • Accepted: 08 March 2022 • Published Online: 21 March 2022

**Md Abu Jafar Rasel, Sergei P. Stepanoff, Maxwell Wetherington, et al.**



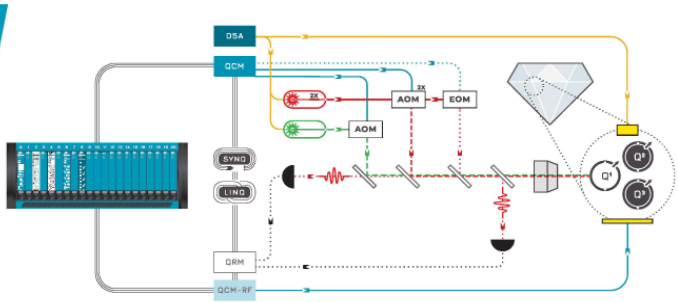

Applied Physics Letters ARTICLE scitation.org/journal/apl

# Thermo-mechanical aspects of gamma irradiation effects on GaN HEMTs

Cite as: Appl. Phys. Lett. **120**, 124101 (2022); doi: 10.1063/5.0087209
Submitted: 2 February 2022 · Accepted: 8 March 2022 ·
Published Online: 21 March 2022



Md Abu Jafar Rasel,[1] Sergei P. Stepanoff,[2] Maxwell Wetherington,[3] Aman Haque,[1,a)] Douglas E. Wolfe,[2] Fan Ren,[4] and Stephen Pearton[5]

## AFFILIATIONS

[1]Department of Mechanical Engineering, Penn State University, University Park, Pennsylvania 16802, USA
[2]Department of Materials Science and Engineering, Penn State University, University Park, Pennsylvania 16802, USA
[3]Materials Characterization Laboratory, Penn State University, University Park, Pennsylvania 16802, USA
[4]Department of Chemical Engineering, University of Florida, Gainesville, Florida 32611, USA
[5]Department of Material Science and Engineering, University of Florida, Gainesville, Florida 32611, USA

[a)]Author to whom correspondence should be addressed: mah37@psu.edu

## ABSTRACT

We report thermal and mechanical responses accompanying electrical characteristics of depletion mode GaN high electron mobility transistors exposed to gamma radiation up to $10^7$ rads. Changes in the lattice strain and temperature were simultaneously characterized by changes in the phonon frequency of $E_2$ (high) and $A_1$ (LO) from the on-state and unpowered/pinched off reference states. Lower doses of radiation improved electrical properties; however, degradation initiated at about $10^6$ rads. We observed about 16% decrease in the saturation current and 6% decrease in the transconductance at the highest dose. However, a leakage current increase by three orders of magnitude was the most notable radiation effect. We observed temperature increase by 40% and mechanical stress increase by a factor of three at a dose of $10^7$ rads compared to the pristine devices. Spatial mapping of mechanical stress along the channel identifies the gate region as a mechanically affected area, whereas the thermal degradation was mostly uniform. Transmission electron microscopy showed contrast changes reflecting a high vacancy concentration in the gate region. These findings suggest that localized stress (mechanical hotspots) may increase vulnerability to radiation damage by accommodating higher concentration of defects that promote the leakage current.



AlGaN/GaN high electron mobility transistors (HEMTs) are attractive for high-power, high temperature, and high-frequency applications because of their high critical electric field and excellent transport properties compared to conventional Si and GaAs technologies.[1] Key to this technology is the mechanical stress induced channel constituted by a high-density two-dimensional electron gas (2DEG).[2] They have also gained considerable interest for use in radiation-harsh environments because of their higher threshold energy for atomic displacement.[3] The higher power density of these wide bandgap devices implies stronger coupling of electrical behavior with the mechanical and thermal domains. Therefore, performance degradation due to mechanical stress and/or high channel temperature becomes important for device reliability, more so with particle irradiation. However, the majority of the radiation effects' studies to date have focused on the electrical domain. Fundamental phenomena that drive the degradation like thermoelastic stress and vertical electric field or temperature have been studied only for pristine devices.[4,5] Radiation induced effects in GaN devices, including single event effects and total dose, have also been investigated significantly over the last ten years, concentrating on mostly assessing the changes in electrical parameters.[6] Spatial mapping of radiation vulnerable regions is a relatively newer concept, which has shown that single event effects not only depend on the high electric field regions but also depend on defect or trap distribution over the channel.[7] This provides the motivation for this study, where we explore the impact of gamma irradiation on electrical parameters as a function of the dose level with simultaneous measurement and comparison of mechanical stress and thermal behavior before and after radiation.

Radiation damage mechanisms vary by radiation type, fluence and total dose, energy and temperature, as well as the carrier density and bond energy in material specific heterostructures, unintentional impurity content, and dislocation density in the active region.[8,9] The effect of gamma irradiation on GaN HEMTs is complex and often equivocal in the literature.[10–13] Subtle differences in the device

structure[14,15] and preexisting trap density might cause such variations. When gamma rays are incident on matter, they primarily interact with electrons and may get absorbed, scattered, or produced electron–positron pairs.[16] When they interact with weakly bound electrons, they lose part of their energy in freeing electrons and may be scattered. The electrons generated through interactions of gamma rays with the material are known as Compton electrons. These, in turn, can create Frenkel pairs and defect clusters, which can migrate, recombine, or form complexes within materials.[17,18] Both negative[10,12,15] and positive[13,15,19,20] threshold voltage shifts have been reported in the literature after gamma irradiation. Moreover, an increase in the drain saturation current, 2DEG sheet concentration, and mobility has been observed up to certain doses,[10,13] and at higher doses, significant decreases (up to 60%) in current and other transport characteristics were reported.[18,20]

This study is motivated by the inherent coupling of mechanical stress with electrical and thermal characteristics in GaN-based systems. In particular, we seek to answer how thermal/mechanical stress is changed spatially across the channel when radiation induced defects are present. Thermal degradation is already a recognized performance bottleneck in high-power density devices due to self-heating during operation. Radiation-induced mechanical stress may degrade both thermal and electrical transport by adversely altering both electron and phonon density and mobility during high voltage operation.[21] Since the phonon frequency is altered by both lattice strain and temperature, we adopt a micro-Raman spectroscopy technique that measures the changes in the phonon frequency of $E_2$ (high) and $A_1$ (LO) from the on-state and unpowered/pinched off reference states to decouple and measure the in-plane stress and temperature simultaneously.[5]

Commercially available (CGH60008D, Wolfspeed) dies were irradiated at room temperature to cobalt-60 $\gamma$-doses of $10^5$, $5 \times 10^5$, $10^6$, $5 \times 10^6$, and $10^7$ rads at the Radiation Science and Engineering Center at Penn State University. Samples were fixed within a 4 in. Ø × 4 in. tall iso-dose region inside the gamma cell and irradiated at a NIST traceable certified dose rate of 180 krad/h. The layer structure reported by the manufacturer included a ≈ 20 nm $Al_{0.22}Ga_{0.78}N$ barrier, ≈1 nm thick AlN interlayer, 1.4 $\mu$m GaN buffer, and 100 $\mu$m 4H–SiC substrate with a gate length of $L_g = 0.25\ \mu$m. DC characterization was performed with a temperature-controlled semiconductor parameter analyzer (Formfactor 11000). Micro-Raman measurements were performed using a Horiba LabramHR Evolution with a 532 nm ULF (ultra-low frequency) equipped with 2048 × 512 pixels back illuminated liquid nitrogen cooled InGaAs array detector. For higher spectral resolution, an 1800 g/mm grating was used along with a 100×, NA = 0.9 objective lens to focus the laser excitation on the sample and collect the Raman scattered light resulted in a laser lateral spot size of <1.0 $\mu$m. Measurements were taken in the Raman backscattering configuration with unpolarized detection, enabling the $A_1$ (LO) and $E_2$ (high) phonon modes of GaN to be measured simultaneously. Raman maps were recorded with a step interval of 0.25 $\mu$m across the device channels, and an array of 34 × 3 points scanned. Using a marker on the sample, the Raman maps were recorded in the same location during *in situ* biasing experiments. Each line scan across the device channel was then analyzed to provide the mean and variance of the Raman peak shift at each position along the channel. Peak positions were determined by peak fitting the Raman spectra using a Lorentzian peak profile using the LabSpec6 software.

Figure 1(a) shows the effect of radiation dosage on the drain current ($I_{DS}$) at zero gate voltage ($V_g$). The initial (up to $10^6$ rad) enhancement in output is attributed to relaxation of the elastic strain, leading to higher mobility in AlGaN/GaN heterostructures where the 2DEG is formed.[11,22] Furthermore, low dose $\gamma$ irradiation creates nitrogen vacancies, which act like a donor and may contribute electrons in the channel, which increase $I_{DS}$.[10,23] Similar findings have been reported by Lee *et al.*[24] and Vitusevich *et al.*[11] and attributed to an increase in the minority carrier lifetime and carrier diffusion length. However, instead of their reported negative shift in the threshold voltage with higher dose, we observed positive shift (from −3.1 to −2.97 V) caused by the introduction of negatively charged traps in the AlGaN barrier or in the GaN buffer. The largest change was observed for the gate leakage current, which degraded by ∼3000 times at the $10^7$ rad dose. The saturation drain current, threshold voltage, leakage current at −4 V, and maximum transconductance as a function of the radiation dose are presented in Table I. At $10^7$ rads, the drain saturation current decreased by 16% at zero $V_g$, while 50% reduction in $I_{DS}$ was observed after $1.2 \times 10^8$ rad gamma irradiation.[20] The 2DEG carrier density ($n_s$) in the channel was estimated from the I–V characteristic and decreased by 10% after $10^7$ rad doses. The differences in the carrier density and drain saturation current indicate that not only carrier density but also carrier mobility has decreased in the channel.[25]

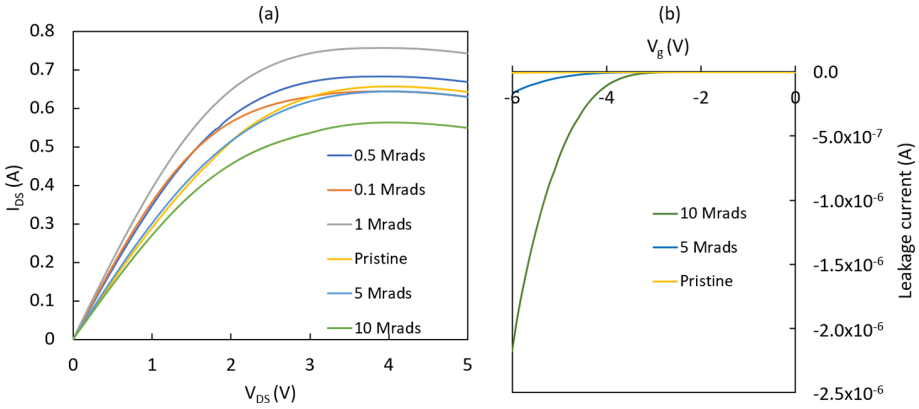


**FIG. 1.** (a) Effect of gamma irradiation doses at zero gate voltage. (b) Gate to source leakage current for three doses.

**TABLE I.** Saturation drain current, threshold voltage, leakage current at −4 V, and maximum transconductance as a function of the irradiation dose.

| | Saturation drain current ($I_{DS}$) (A) | Threshold voltage ($V_{th}$) (V) | Leakage current (A) | Maximum transconductance ($G_m$) (mS) |
|---|---|---|---|---|
| Pristine | 0.64 | −3.10 | $-3.51 \times 10^{-11}$ | 27.5 |
| $5 \times 10^6$ rad | 0.62 | −2.82 | $-4.9 \times 10^{-9}$ | 26.8 |
| $10^7$ rad | 0.54 | −2.82 | $-1.05 \times 10^{-7}$ | 25.8 |

The maximum transconductance ($G_m$) was decreased by 6% after $10^7$ rad doses. A 25% decrease in $G_m$ was reported before $6 \times 10^8$ rad gamma irradiation.[8] The observed decrease in transconductance ($G_m$) can be attributed to the large number of defect sites, which outweighs the gamma-radiation induced carrier generation and decreases in the effective channel doping through introduction of deep electron traps.[26]

The significant degradation in terms of the leakage current may have impact radiation sensitivity, wherein we hypothesize that the lattice defect would play a key role. Defects, such as vacancies or dislocations, would develop to relax the high mechanical stresses in the lattice and interfaces, promoting the leakage current. This would impact both electron and phonon transport, and higher temperatures are expected as well. We performed micro-Raman spectroscopy utilizing the peak shift of two phonon modes [$E_2$ (high) and $A_1$ (LO)] to simultaneously determine operating temperature and stress. Furthermore, during the ON state of the device, the high electric field and temperature are generated, which also contribute to overall strain. As the vertical electric field is approximately equal in both the pinched off state and ON state, the electric field can be decoupled by taking pinch-off as a reference state and $E_2$ (high) and $A_1$ (LO) modes are sufficient to measure two unknowns, i.e., temperature and stress. By measuring the $E_2$ (low) phonon mode, an electric field can be derived but the $E_2$ (low) mode has low frequency (140–145 $cm^{-1}$) and low intensity, which makes it difficult to fit during analysis. Shifts in Raman peaks can be expressed by two linear equations

$$(\omega - \omega_0)_{E_2(high)} = A_{E_2(high)}(T - T_0) + K_{E_2(high)}\sigma, \quad (1)$$

$$(\omega - \omega_0)_{A_1(LO)} = A_{A_1(LO)}(T - T_0) + K_{A_1(LO)}\sigma, \quad (2)$$

where $\omega$ and $\omega_0$ are the Raman peak position of the nth phonon mode in the operating state and a reference condition (pinched off state), respectively, $(T - T_0)$ is the temperature difference between those two states assuming negligible temperature rise in the pinched off state [$V_g < V_{th}$ (threshold voltage)] due to the very low dissipated power, A is the temperature coefficient, K is the biaxial stress coefficient, and $\sigma = (\sigma_x + \sigma_y)/2$ is defined as average stress or in plane stress in the c plane stimulated by the thermoelastic effect. The temperature and stress are obtained from

$$\begin{bmatrix} \Delta T \\ \sigma \end{bmatrix} = \begin{bmatrix} A_{E_2(high)} & K_{E_2(high)} \\ A_{A_1(LO)} & K_{A_1(LO)} \end{bmatrix}^{-1} \begin{bmatrix} \Delta\omega_{E_2(high)} \\ \Delta\omega_{A_1(LO)} \end{bmatrix}. \quad (3)$$

This method is known as the linear peak fit method[4,5] and is advantageous over other existing methods in terms of experimental time and accuracy. Coefficients A and K for both phonon modes are taken from the literature,[4,5,27] where their values are measured and compared by different methods like XRD, Raman, photoluminescence (PL), *Ab initio* (DFT), etc., and these values agree within 10% accuracy or better. The pinched off state and on state are at $V_g = -4$ V and $V_g = -1$ V, respectively, and $V_{DS}$ is kept fixed at 5 V. At the on-state, dissipated power from pristine and $10^7$ rad irradiated devices are 2.25 and 2 W, respectively.

Figure 2(a) shows the top view of the device. One device under preirradiated condition and another device under postirradiated condition are used for the experiment. As these devices are commercially made and their electrical parameters are consistent, we used one device for each experiment. However, to confirm repeatability in our measurements, we have taken all the measurements three times. The error bar is calculated from the uncertainty in the measurement data along with the uncertainty in the coefficient. The Raman signals are very strong across the channel except over the gate region, where the gate metal (Au/Ni) is deposited. Both the $A_1$ (LO) and $E_2$ (high) phonon modes shift to lower frequencies when operating the device, primarily due to self-heating. The highest temperature gradient is found near the vicinity of the gate region, where the highest concentration of the electrical field appears, but irradiated devices show a larger temperature

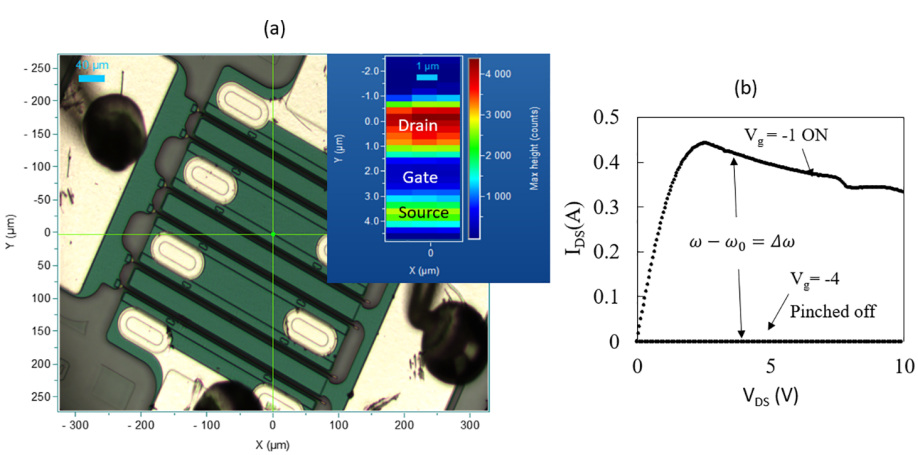


**FIG. 2.** (a) Top view of the commercial AlGaN/GaN HEMTs' device with the inset showing the intensity map across the channel. (b) Output drain current and drain voltage characteristics at the pinched off state ($V_g = -4$ V) and ON state ($V_g = -1$ V). Peak shifts were measured at 5 V $V_{DS}$ for best signal.

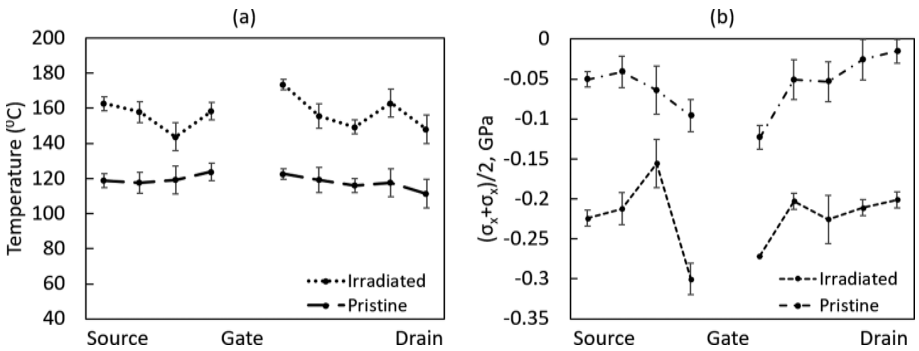


**FIG. 3.** (a) Temperature and (b) mechanical stress profile at fixed drain bias (5 V) on a pristine and $10^7$ rad exposed HEMT.

across the GaN layer as shown in Figure 3(a). The gradient is almost similar for both doses with only the absolute values being increased, which may suggest uniform damage across the channel. Defects introduced by irradiation can scatter charge carriers and elevate temperature during operation. In the same manner, the mechanical stress reaches its highest value near the gate with a value about −0.3 GPa. Figure 3(b) shows that the average induced stress is higher on the drain side of the gate than the source side. Similar measurements on pristine devices have been performed previously with different bias conditions; however, with the same dissipated power, the temperature rise near the gate terminal is consistent with their findings.[4,5] They also reported a linear relationship of temperature and stress with dissipated power, which is a concern as it may restrict the use of the GaN HEMTs at high power in harsh radiation environments. Our results indicate that the channel has developed more scattering centers after being irradiated, which explains an increase in the leakage current.

As shown in Fig. 3, both temperature and mechanical stress are maximum at the drain side of the gate region, indicating the vulnerability of this region to incoming radiation. This finding can explain the three orders of magnitude increase in the gate leakage current. Further evidence of gate region vulnerability is shown in Fig. 4, where a bright field transmission electron microscope image is shown for a radiation dose of $10^7$ rad. The threading dislocations are seen over the entire channel length because of the uniform radiation exposure. However, the higher mechanical stress at the gate region may lead to a clearly discernible change of contrast (below the gate). For the same specimen thickness, regions with higher vacancy density are expected to scatter more transmission electrons as the electron beam traverses the specimen and, thus, appears darker in a bright field image. We have observed this effect in heavy ion irradiated GaN HEMTs previously.[28]

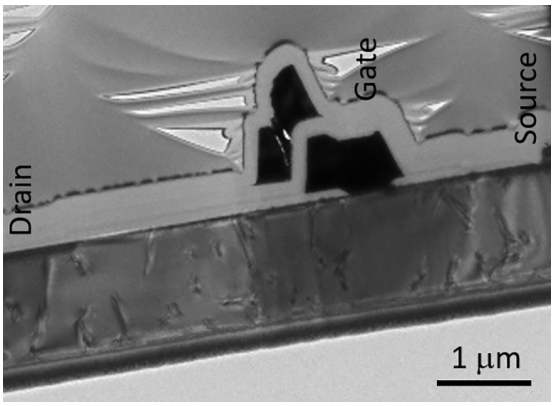


**FIG. 4.** Bright-field TEM image showing increased contrast at the gate region arising from electron scattering due to increased vacancy density.

In summary, we characterized thermal and mechanical effects of gamma radiation on GaN HEMTs. Decreases in the drain saturation current and maximum transconductance, positive shifts in the threshold voltage, and increases in the leakage current were found for $5 \times 10^6$ and $10^7$ rad irradiated devices, which indicate generation of point defects and at higher doses, carrier scattering became pronounced, leading to the degradation of carrier mobility. Micro-Raman studies revealed higher channel temperature and mechanical stress during the ON state after the sample was irradiated to $10^7$ rad. Three orders of magnitude increase in the gate leakage current was observed, which could be attributed to the increased stress (and, hence, vacancy density) at the gate region. This was confirmed with transmission electron microscopy. These findings lead to the insight that stress localization in electronic devices increases vulnerability to radiation damage. Regions with higher stresses will contain higher concentration of defects not only to promote charge generation (in the case of ionizing radiation) but also to enhance transport as reflected by the relative magnitude of the leakage current.

This work was funded by the Defense Threat Reduction Agency (DTRA) as part of the Interaction of Ionizing Radiation with Matter University Research Alliance (IIRM-URA) under Contract No. HDTRA1-20-2-0002. The content of the information does not necessarily reflect the position or the policy of the federal government, and no official endorsement should be inferred. A.H. also acknowledges support from the U.S. National Science Foundation (ECCS No. 2015795). The work at UF was also supported by NSF DMR via No. 1856662 (James Edgar).

## AUTHOR DECLARATIONS

### Conflict of Interest

The authors have no conflicts to disclose.

## DATA AVAILABILITY

The data that support the findings of this study are available from the corresponding author upon reasonable request.

## REFERENCES


[1]U. K. Mishra, P. Parikh, and Y.-F. Wu, Proc. IEEE **90**(6), 1022 (2002); J. W. Chung, W. E. Hoke, E. M. Chumbes, and T. Palacios, IEEE Electron Device Lett. **31**(3), 195 (2010); Y.-F. Wu, M. Moore, A. Saxler, T. Wisleder, and P. Parikh, paper presented at 2006 64th device research conference, 2006; Y.-F. Wu, D. Kapolnek, J. P. Ibbetson, P. Parikh, B. P. Keller, and U. K. Mishra, IEEE Trans. Electron Devices **48**(3), 586 (2001).

[2]O. Ambacher, J. Smart, J. R. Shealy, N. G. Weimann, K. Chu, M. Murphy, W. J. Schaff, L. F. Eastman, R. Dimitrov, and L. Wittmer, J. Appl. Phys. **85**(6), 3222 (1999).

[3]A. Ionascut-Nedelcescu, C. Carlone, A. Houdayer, H. J. Von Bardeleben, J.-L. Cantin, and S. Raymond, IEEE Trans. Nucl. Sci. **49**(6), 2733 (2002).

[4]S. Choi, E. R. Heller, D. Dorsey, R. Vetury, and S. Graham, IEEE Trans. Electron Devices **60**(6), 1898 (2013).

[5]K. R. Bagnall, E. A. Moore, S. C. Badescu, L. Zhang, and E. N. Wang, Rev. Sci. Instrum. **88**(11), 113111 (2017).

[6]S. Onoda, A. Hasuike, Y. Nabeshima, H. Sasaki, K. Yajima, S.-i. Sato, and T. Ohshima, IEEE Trans. Nucl. Sci. **60**(6), 4446 (2013); M. Rostewitz, K. Hirche, J. Lätti, and E. Jutzi, IEEE Trans. Nucl. Sci. **60**(4), 2525 (2013); S. Kuboyama, A. Maru, H. Shindou, N. Ikeda, T. Hirao, H. Abe, and T. Tamura, IEEE Trans. Nucl. Sci. **58**(6), 2734 (2011).

[7]A. Khachatrian, N. J. H. Roche, S. P. Buchner, A. D. Koehler, J. D. Greenlee, T. J. Anderson, J. H. Warner, and D. McMorrow, IEEE Trans. Nucl. Sci. **63**(4), 1995 (2016).

[8]S. J. Pearton, Y.-S. Hwang, and F. Ren, JOM **67**(7), 1601 (2015).

[9]L. Liu, C.-F. Lo, Y. Xi, Y. Wang, F. Ren, S. J. Pearton, H.-Y. Kim, J. Kim, R. C. Fitch, and D. E. Walker, Jr., J. Vacuum Sci. Technol., B **31**(2), 022201 (2013); T. Roy, E. X. Zhang, Y. S. Puzyrev, D. M. Fleetwood, R. D. Schrimpf, B. K. Choi, A. B. Hmelo, and S. T. Pantelides, IEEE Trans. Nucl. Sci. **57**(6), 3060 (2010); A. Y. Polyakov, S. J. Pearton, P. Frenzer, F. Ren, L. Liu, and J. Kim, J. Mater. Chem. C **1**(5), 877 (2013).

[10]O. Aktas, A. Kuliev, V. Kumar, R. Schwindt, S. Toshkov, D. Costescu, J. Stubbins, and I. Adesida, Solid-State Electron. **48**(3), 471 (2004).

[11]S. A. Vitusevich, N. Klein, A. E. Belyaev, S. V. Danylyuk, M. V. Petrychuk, R. V. Konakova, A. M. Kurakin, A. E. Rengevich, A. Y. Avksentyev, and B. A. Danilchenko, Phys. status Solidi A **195**(1), 101 (2003).

[12]S. A. Vitusevich, A. M. Kurakin, R. V. Konakova, A. E. Belyaev, and N. Klein, Appl. Surf. Sci. **255**(3), 784 (2008).

[13]C. Schwarz, A. Yadav, M. Shatkhin, E. Flitsiyan, L. Chernyak, V. Kasiyan, L. Liu, Y. Y. Xi, F. Ren, and S. J. Pearton, Appl. Phys. Lett. **102**(6), 062102 (2013).

[14]K. Ahn, Y. K. Ooi, F. Mirkhosravi, J. Gallagher, A. Lintereur, D. Feezell, E. K. Mace, and M. A. Scarpulla, J. Appl. Phys. **129**(24), 245703 (2021); G. Wenping, C. Chi, D. Huantao, H. Yue, Z. Jincheng, W. Chong, F. Qian, and M. Xiaohua, J. Semicond. **30**(4), 044002 (2009).

[15]P. J. Martínez, E. Maset, P. Martín-Holgado, Y. Morilla, D. Gilabert, and E. Sanchis-Kilders, Materials **12**(17), 2760 (2019).

[16]G. Nelson and D. Reilly, NUREG/CR-5550, LAUR-90-732 (Los Alamos National Laboratory, 1991).

[17]J. Kim, F. Ren, G. Y. Chung, M. F. MacMillan, A. G. Baca, R. D. Briggs, D. Schoenfeld, and S. J. Pearton, Appl. Phys. Lett. **84**(3), 371 (2004).

[18]Y.-H. Hwang, Y.-L. Hsieh, L. Lei, S. Li, F. Ren, S. J. Pearton, A. Yadav, C. Schwarz, M. Shatkhin, and L. Wang, J. Vacuum Sci. Technol., B **32**(3), 031203 (2014).

[19]H.-Y. Kim, J. Kim, L. Liu, C.-F. Lo, F. Ren, and S. J. Pearton, J. Vacuum Sci. Technol., B **31**(5), 051210 (2013).

[20]M. P. Khanal, B. Ozden, K. Kim, S. Uprety, V. Mirkhani, K. Yapabandara, A. C. Ahyi, and M. Park, J. Vacuum Sci. Technol., B **35**(3), 03D107 (2017).

[21]Y. Zhang, I. P. Smorchkova, C. R. Elsass, S. Keller, J. P. Ibbetson, S. Denbaars, U. K. Mishra, and J. Singh, J. Appl. Phys. **87**(11), 7981 (2000).

[22]M. R. Hogsed, Y. K. Yeo, M. Ahoujja, M.-Y. Ryu, J. C. Petrosky, and R. L. Hengehold, Appl. Phys. Lett. **86**(26), 261906 (2005); C. Sharma, A. K. Visvkarma, R. Laishram, A. Malik, K. Narang, S. Vinayak, and R. Singh, Semicond. Sci. Technol. **34**(6), 065024 (2019).

[23]G. A Umana-Membreno, J. M. Dell, T. P. Hessler, B. D. Nener, G. Parish, L. Faraone, and U. K. Mishra, Appl. Phys. Lett. **80**(23), 4354 (2002); A. Chatterjee, S. K. Khamari, S. Porwal, S. Kher, and T. K. Sharma, J. Appl. Phys. **123**(16), 161585 (2018).

[24]J. Lee, A. Yadav, M. Antia, V. Zaffino, E. Flitsiyan, L. Chernyak, J. Salzman, B. Meyler, S. Ahn, and F. Ren, Radiat. Eff. Defects Solids **172**(3–4), 250 (2017).

[25]A. M. Kurakin, S. A. Vitusevich, S. V. Danylyuk, H. Hardtdegen, N. Klein, Z. Bougrioua, B. A. Danilchenko, R. V. Konakova, and A. E. Belyaev, J. Appl. Phys. **103**(8), 083707 (2008).

[26]B. Luo, J. W. Johnson, F. Ren, K. K. Allums, C. R. Abernathy, S. J. Pearton, A. M. Dabiran, A. M. Wowchack, C. J. Polley, and P. P. Chow, Appl. Phys. Lett. **80**(4), 604 (2002).

[27]S. Choi, E. Heller, D. Dorsey, R. Vetury, and S. Graham, J. Appl. Phys. **113**(9), 093510 (2013).

[28]Z. Islam, A. L. Paoletta, A. M. Monterrosa, J. D. Schuler, T. J. Rupert, K. Hattar, N. Glavin, and A. Haque, Microelectron. Rel. **102**, 113493 (2019).